

MASSIVE STRUCTURE MONITORING: RELEVANCE OF SURFACE STRAIN MEASUREMENT

Maxime Boucher¹, Matthieu Briffaut¹, Frédéric Dufour^{1,2}

¹ Univ. Grenoble Alpes, 3SR, F-38000 Grenoble, France
CNRS, 3SR, F-38000 Grenoble, France

² Chair Professor PERENITI

e-mail: maxime.boucher@3sr-grenoble.fr, webpage: <http://3sr-grenoble.fr>

ABSTRACT

Most of large civil engineering concrete structures have been instrumented for decades with embedded sensors. To prevent the eventual loss of data, complementary instrumentation of external surface has recently been deployed.

This new instrumentation can take different forms but in all cases, to avoid damaging the structure, it will be only superficially anchored. Near the outer surfaces, thermo-hydro-mechanical concrete behaviour is more sensitive to varying environmental conditions than in the centre of the structures. Therefore, the strain measured near the outer surfaces is not identical to the strain measured by embedded sensors. Consequently the methods of classical physical-statistical analysis must be reviewed.

Using a thermo-hydro-mechanical finite element modeling calibrated on a representative concrete and applied on a current part of a thick structure, this work confirms a dependence of strain on the depth. First results show that the depth impact affects both kinetic and amplitude strain.

Keywords.

Thermo-Hydro-Mechanical Behaviour, Concrete, Massive Structure, Variable Environmental Conditions, Surface Monitoring

INTRODUCTION

For nearly 80 years, most of large civil engineering concrete structures are instrumented with vibratory strain gauge. On some structures such as confinement vessels of nuclear power plants (highly prestressed), operators have to cope with the loss of signal from some sensors. This can be explained by several reasons including a default in the electrical system that excite the wire or by the excess of frequency limit measurement due for instance to important creep strains (*Simon and Courtois, 2011; Simon et al. 2013*). Most of these sensors have been embedded in the concrete during construction and are thus irreplaceable. To overcome this loss of information, one of the

solutions is to replace these defective embedded sensors by surface sensors (Figure 1).

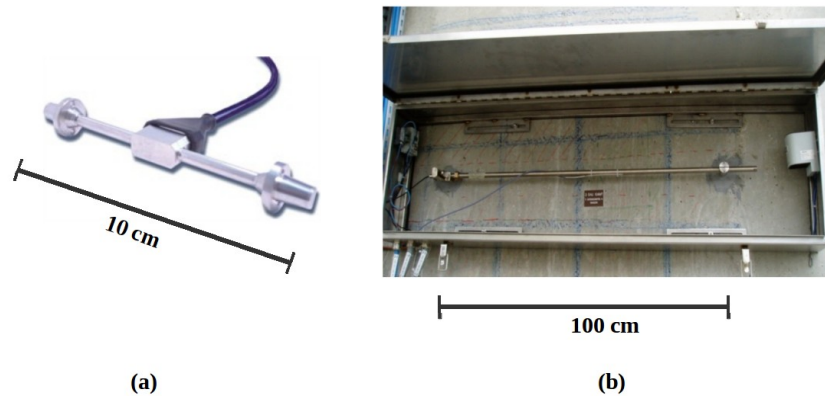


Figure 1: Embedded strain sensor (a) and surface strain sensor (b).

Nevertheless, unlike central strain (far from outer surface), skin strain (near outer surfaces) is strongly affected by the environmental condition variations. Temperature and humidity cycles (daily and seasonal) generate thermo-hydric variations of volume. Other phenomena such as sunshine, rain or wind, also disrupt these two main fields. Finally, characteristic times and so influence depths of these phenomena are very different. For these reasons, the analysis of this new data is more complex than embedded measures for which usual statistical analysis methods exist.

The aim of the present contribution is to compare the strain evolution through the depth in thick structure. This can be considered as a first step toward the complete definition of a space and time transfer functions between both strain vs time signals.

For this purpose, a visco-elastic finite element model able to represent thermo-hydro-mechanical behaviour of concrete submitted to variable thermo-hydric boundary conditions is presented in the first part. Then, the calibration of the material constitutive parameters on laboratory tests is detailed. Finally, the strains at different depths from a simulation over thirty years on a current part of containment enclosure submitted to thermo-hygrometric variations are analysed.

NUMERICAL MODEL

Numerical strategy.

To be applicable to major civil engineering thick structures, the numerical model must account for thermal and hydric variation effects on strains. Thermo-mechanical (*Arthanari and Yu, 1967 ; Seki and Kawasumi, 1972 ; Kommendant et al, 1976*), hydro-mechanical (*Wittmann, 1970 ; Wittmann, 1973*) and thermo-hydric (*Caré, 2008*) chaining are retained. In contrast, the effects of mechanical strains on thermal and hydric

properties (*Lassabatere et al, 1997*) and the modification of heat and water diffusivity due to cracked skin are neglected. Finally, for ageing structures, hydration reaction is supposed finished.

Complete simulations are carried out using *Code_Aster* by chaining three calculations: thermal field, hydric field and mechanical strains. Constitutive models adopted are for the most part empirical although based on physical approaches.

Thermal field.

Thermal field is assumed to be governed by a conventional linear heat equation with convective boundary conditions (Neumann type):

$$\begin{cases} \rho C_{th} \dot{T} = k_{th} \Delta T \\ \varphi_{th} = h_{th} (T - T_{\infty}) \end{cases} \quad (1)$$

Specific heat capacity ρC_{th} , thermal conductivity k_{th} and heat transfer coefficient h_{th} (taking into account convection and radiation) are taken constant during all the calculation.

Hydric field.

Drying process is modeled by a nonlinear diffusion equation involving a diffusion coefficient (non-linear function of water content) usually written as:

$$\dot{C} = \nabla [D(C, T) \nabla T] \quad (2)$$

Several authors have proposed various relationships between drying coefficient and water content. The expression used, proposed by Granger (1995), is composed of the drying coefficient proposed by Mensi (1988) and the temperature dependence given by Bazant (1972):

$$D(C, T) = a e^{bc} \frac{T}{T_0} e^{\frac{-Q}{R} (\frac{1}{T} - \frac{1}{T_0})} \quad (3)$$

The coefficients a, b and the activation energy Q of Arrhenius' law are supposed to be constant. T_0 represents the reference temperature.

The calculation of drying is done by means of water content, although boundary conditions are prescribed in relative humidity. The isotherm between relative humidity of concrete and water content must be entered. In this study, the hysteresis existing between sorption and desorption cycles is neglected and the isotherm is supposed linear in the humidity range between 40% and 100%. Therefore, the used isotherm function is:

$$C(h) = \frac{C_{eq}[h_0 - h] - C_0[h - h_{eq}]}{h_0 - h_{eq}} \quad (4)$$

where h_0 , C_0 are the relative humidity and initial moisture content and h_{eq} , C_{eq} are the relative humidity and water content at equilibrium.

The convective boundary condition used involves a water exchange coefficient h_{dr} which is assumed constant:

$$\varphi_{dr} = h_{dr}[C - C(h_{air})] \quad (5)$$

By analogy with nonlinear thermal calculation, water field is obtained using the nonlinear thermal module of *Code_Aster*.

Mechanical field.

This study focuses on operating structures during service life. Consequently damage rate is assumed to be low and a simple elastic model is used.

Under the assumption of small strains, the total strain tensor is assumed to be the sum of five tensors: elastic strain (ϵ_{El}), thermal strain (ϵ_{Th}), drying shrinkage strains (ϵ_{DS}), basic creep strains (ϵ_{BC}) and drying creep strains (ϵ_{DC}):

$$\underline{\epsilon}_{tot} = \underline{\epsilon}_{El} + \underline{\epsilon}_{Th} + \underline{\epsilon}_{DS} + \underline{\epsilon}_{BC} + \underline{\epsilon}_{DC} \quad (6)$$

- The thermal strain is assumed to be proportionnal to the temperature change: $\underline{\epsilon}_{El} = \alpha_{Th} \cdot \dot{T} \cdot \underline{1}$.
- For the calculation of drying shrinkage, a phenomenological model assuming proportionality with water variation content is used: $\underline{\epsilon}_{DS} = \alpha_{DS} \cdot \dot{C} \cdot \underline{1}$.
- The basic creep model is based on simple rheological models: an elastic body, a linear Kelvin-Voigt for modeling reversible creep and a Maxwell unit with a nonlinear viscosity to model the long time creep. The model also assumes complete decoupling between the spherical and deviatoric components. Both of these chains are however equivalent in their construction. A linear dependance with internal relative humidity is included.
- The model, proposed by Bazant (1985), is assumed to be a linear relation with strain and internal relative humidity variations: $\underline{\epsilon}_{DC} = \alpha_{DC} \cdot |\dot{h}| \cdot \underline{\sigma}$.

CALIBRATION

The numerical model presents 20 material parameters to be determined. For this, laboratory tests on specimens formed by a representative concrete of nuclear power plant are used. These tests are of two types:

- A first test campaign on 4 specimens of dimensions 25x50cm subjected to axial compression cycles from 0 to 12 MPa.
- A second test campaign on 14 specimens of dimensions 16x100cm subjected to various conditions:
 - Non-drying weight loss (1 specimen)
 - Drying weight loss (1 specimen)
 - Non drying shrinkage (3 specimens)

- Drying shrinkage (3 specimens)
- Non drying creep (3 specimens)
- Drying creep (3 specimens)

Non-drying conditions were ensured by strips of self-adhesive aluminium. The temperature was maintained near to 20°C. The relative humidity has oscillated between 50% and 70%. All strain measurements were carried out with inductive sensors located outside the specimens.

Since the variability between specimen responses from the second campaign was low, only one out of the three (for shrinkage and creep tests) was carried out up to the end of the campaign. The model was calibrated with these last specimens.

For confidentiality reasons, the experimental results will be normalized and the parameter values will not be provided.

Thermal field.

The thermal diffusion and the specific capacity cannot be measured out of these tests. Thus, their retained values were obtained from the literature. It is the same for the heat exchange coefficient.

Hydric field.

Before calibrating the drying model, the sorption-desorption isotherm of the concrete must be determined in order to translate the boundary conditions (known in relative humidity of the surrounding air) in concrete water content.

Initial relative humidity of concrete (h_0) is taken equal to 100% (saturated) and equal to the average of the relative humidity in the air during all the test at equilibrium (h_{eq}).

The initial water content (C_0) is defined as the amount of water used to make concrete minus the water used in hydration reaction (*Granger 1995*). The final water content (C_{eq}) is obtained by extrapolating the weight loss curve to infinity.

Finally, the drying model was calibrated on the drying mass loss test. The water exchange coefficient and the coefficient b (Equation 3) from diffusion coefficient have been fixed to reference values from the literature. Only the coefficient a from diffusion coefficient has been calibrated. The comparison between the experimental points and the numerical curve is presented in Figure 2a.

Elastic strain.

Measurements from the first campaign were used to determine the Young's modulus of concrete studied. A linear regression of the stress-strain curves (Figure 3a) allows to determine an average Young's modulus for these four specimens.

Since only axial strains were measured, the Poisson's ratio could not be determined. Therefore a standard value for concrete is used.

Thermal strain.

No thermal expansion test was made. But peaks of temperature up to 25°C were

measured during the campaign. These variations have been felt on shrinkage and creep tests. These thermal anomalies have been used to calibrate the thermal expansion coefficient.

The analysis of the experimental results yields an increase of strain with temperature amplitude (Figure 3b). A linear regression of these points gives direct access to the thermal expansion coefficient α_{Th} .

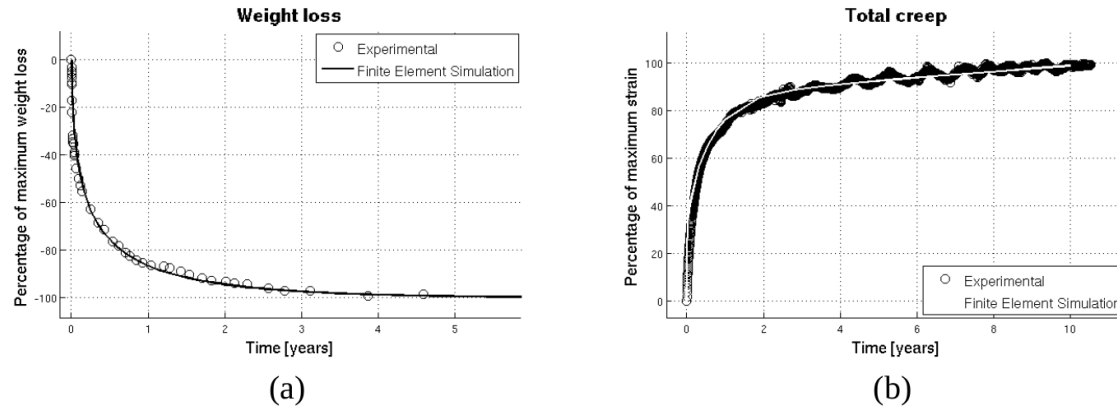


Figure 2: Calibration of the thermo-hydro-mechanical model. Numerical simulations: weight loss (a) and total creep (b).

Drying shrinkage.

The drying shrinkage strain is assumed to be proportional to the variation of water content. Therefore, only one parameter must be identified (α_{DS}). Autogenous shrinkage was estimated at short-term from non-drying weight loss. Then, it was subtracted to drying shrinkage test in order to obtain the drying shrinkage. The obtained curve is not exactly linear at the beginning (Figure 3c). Indeed, at the start of drying, the high tensile stress located near the exchange surfaces creates skin cracking, which relaxes the stress. A linear regression of the central portion of the curve allows the calibration of the drying shrinkage parameter. Numerically, the strain obtained will be greater than the experimental measurement. However both kinetic and amplitude related to relative humidity cycles will be respected.

Drying creep.

It was decided arbitrarily to calibrate drying creep before basic creep (since it has only one parameter). Experimental curve of drying creep was obtained by subtracting non-drying creep and drying shrinkage to the drying creep test. Since drying creep was assumed proportional to the stress and the relative humidity variation, drying creep values were divided by the applied stress. Meanwhile, the mass loss was translated into relative humidity thanks to the sorption-desorption isotherm.

A quasi-linear increase of drying creep with relative humidity variation is highlighted by

the analysis of experimental results in Figure 3d. Again, as for drying shrinkage, the resulting curve is not perfectly linear in its ends. For the beginning, explanations may be the same than in the case of drying shrinkage. For the long term, the permeability of desiccation protection is probably involved. It was found that after a few years, the mass loss from non-drying test increased significantly. Consequently, in our approach, by subtracting non-drying creep and drying shrinkage to drying creep, drying shrinkage is removed twice which explains the decrease at the end of the curve. That is why, drying creep parameter is identified by linear regression of the central portion of the experimental curve only (Figure 3d).

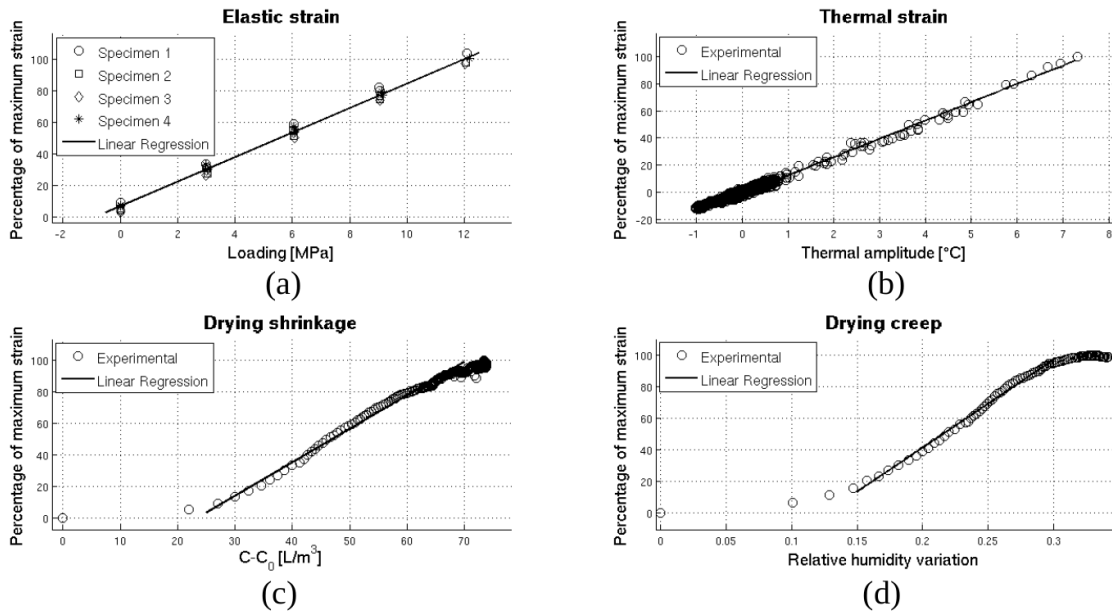


Figure 3: Calibration of the thermo-hydro-mechanical model. Linear regressions: elastic strain (a), thermal strain (b), drying shrinkage (c) and drying creep (e).

Basic creep.

Finally, basic creep is calibrated on the total creep test, taking into account the previously calibrated drying creep. Experimental and numerical results are presented in Figure 2b.

SIMULATION METHOD

After a thorough calibration of material parameters for each modeled phenomena, an application to a representative volume of a confinement vessel of a nuclear power plant was achieved. For this simulation, an inner containment wall of a double containment vessel is studied which allows the suppression of the direct effects

of rain, wind and sunshine; only thermal and humidity variations, load and prestressing were selected as thermo-hydro-mechanical boundary conditions.

The mesh of a current portion of containment in three dimensions (width of 2 meters, height of 1.8 meters, thickness of 1.2 meters and internal radius of 21.9 meters), taking into account reinforcements was used (Figure 4).

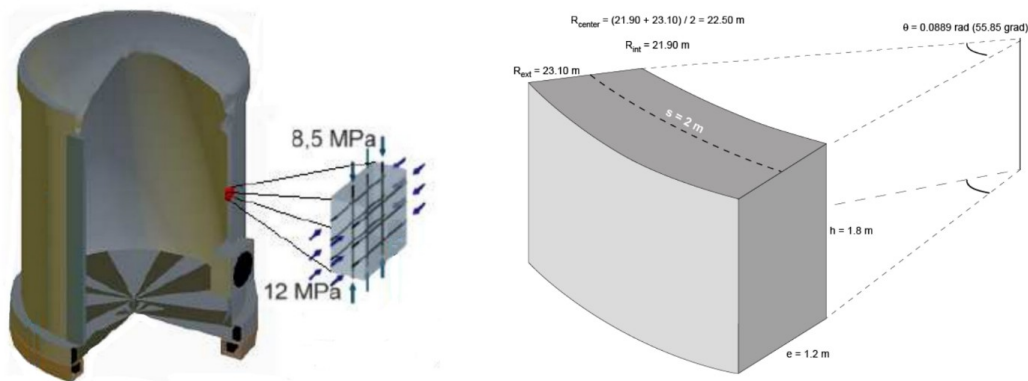


Figure 4: Geometry and dimensions of the studied structure.

The calculation simulates 30 years of service life of the structure. The thermo-hygrometric boundary conditions were created by duplicating periodic temperature and humidity measurements from the studied structure.

In-situ mechanical boundary conditions are represented by the following hypothesis: on the bottom and lateral faces, normal displacements are prohibited and the upper side is forced to remain parallel to the bottom side.

During the first three years, only the structural loading, the thermal and the moisture variations (identical on the inner and outer faces) are taken into account.

At 3.5 years, the vertical and horizontal preloading is added.

At 6 years, the reactor is operating. This yields a change in thermo-hygrometric boundary conditions (different on the inner and outer sides).

At 16 and 26 years, two containment pressure tests are simulated (pressurizing the reactor vessel for 3 days). For that, an overpressure is added on the inner side and an depression is added on the upper face (to represent the vertical stretch of the structure).

RESULTS :

The orthoradial strains obtained numerically on the outer surface and near the center of the structure are presented in Figure 5. Also for confidentiality reasons, the strains are normalized by the absolute value of the center strain at 30 years.

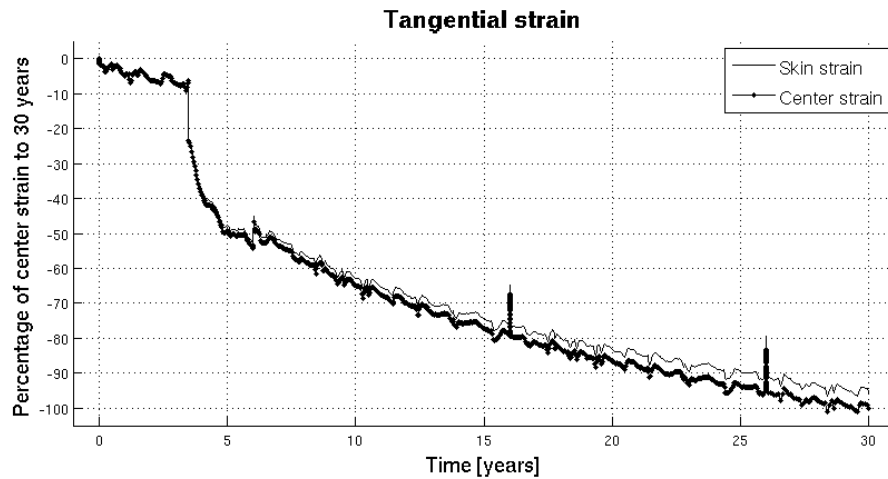


Figure 5: Tangential strain on outer surface and close to center of structure.

On this graph, one can remark that:

- Strain cycles related to thermal variations between the center and the skin are closed to each others.
- Given the thickness of the structure and a very low water diffusivity, in comparison to thermal strain and creep, the drying shrinkage of the concrete is only slightly perturbed by the changes in humidity of the air.
- Before prestressing, both strains observed in skin and in the center are similar. After prestressing the cables, the creep kinetics begin to dissociate: faster in the center (high water content) than at the surface (low water content). After 30 years, this difference is about 5%.

CONCLUSION

The results of this study show that, unlike thermal variations which affect the entire thickness of the structure, creep kinetics are not the same between the center and the surface of the structure. Creep is smaller near the exchange surfaces, where concrete has a lower water content.

Under the hypothesis used in the numerical part, this contribution shows that the strain evolution between the core and the surface of the structure are not exactly the same. This confirms that the identification of a transfer function is necessary between strain measurement at various depth. Given the above results, a simple reduction of the strain depending on the distance to the outer sides could be accurate enough.

Benefiting from a representative structure, built in the same concrete used for the calibration procedure and instrumented with surface strain sensors for several years, this present work will continue with a comparison between simulated strain and measured strain.

Acknowledgments.

Work performed thanks to the support of EDF in context of Chair PERENITI run by the Fondation Partenariale Grenoble INP and using the monitoring data provided by EDF-DTG. Partners responsibility of the Chair cannot in any circumstances be blamed on the grounds of the content of the publication, which is only binding its author.

REFERENCES

- Arthanari S., Yu C.W. (1967). "Creep of concrete under uniaxial and biaxial stresses at elevated temperatures". *Mag. Concrete Res.* 13(60), 149-156.
- Bazant Z.P., Najjar L.J. (1972). "Nonlinear water diffusion in nonsaturated concrete". *Materials and Constructions*, 1972, Vol. 5, 3-20.
- Bazant Z.P., Chern J.C. (1985). "Concrete creep at variable humidity: constitutive law and mechanism". *Matériaux et Constructions*, Vol. 18, n°103, pp 1-20.
- Caré S. (2008). "Effect of temperature on porosity and on chloride diffusion in cement pastes". *Construction and Building Materials* 22, 1560-1573.
- Code_Aster, Électricité De France (EDF), Code_Aster finite element code version 11.5, available at <http://www.code-aster.org>.
- Granger L. (1995). "Comportement différé du béton dans les enceintes de centrales nucléaires: analyse et modélisation". *Laboratoire Central des Ponts et Chaussées*.
- Kommendant G., Polivka M., Pirtz D. (1976). "Study of concrete properties for prestressed concrete reactor vessels". *Rapport technique, Department of Civil Engineering*.
- Lassabaterre T., Torrenti J.-M., Granger L. (1997). "Sur le couplage entre séchage du béton et contrainte appliquée". Pages 331-338.
- Mensi R., Acker P., Attolou A. (1988). "Séchage du béton : analyse et modélisation". *Materials and Structures/Matériaux et Construction*, 1988, 21, 3-12.
- Seki S., Kawasumi M. (1972). "Creep of concrete at elevated temperatures". *Concrete of Nuclear Reactors*, 1:591-638.
- Simon A., Courtois A. (2011). « Structural Monitoring of Prestressed Concrete Containments of Nuclear Power Plants for ageing management ». *Transactions, SmiRT 21*, 6-11 November, 2011, New Delhi, India.
- Simon A., Oukhemanou E., Courtois A. (2013). « Structural Monitoring of Prestressed Concrete Containments of Nuclear Power Plants for ageing management ». *Technical Innovation in Nuclear Civil Engineering – TINCE 2013*, Paris (France), October 23-31, 2013.
- Wittmann F. (1970). « Einfluss des feuchtigkeitsgehaltes auf das kriechen des zementsteines ». *rheologica Acta*, 9(2):282-287.
- Wittmann F. (1973). « Interaction of hardened cement paste and water ». *Journal of the American ceramic society*, 56(8):409-415.